REPORT DOCUMENTATION PAGE

Form Approved OMB NO. 0704-0188

The public reporting burden for this collection of information is estimated to average 1 hour per response, including the time for reviewing instructions, searching existing data sources, gathering and maintaining the data needed, and completing and reviewing the collection of information. Send comments regarding this burden estimate or any other aspect of this collection of information, including suggesstions for reducing this burden, to Washington Headquarters Services, Directorate for Information Operations and Reports, 1215 Jefferson Davis Highway, Suite 1204, Arlington VA, 22202-4302. Respondents should be aware that notwithstanding any other provision of law, no person shall be subject to any oenalty for failing to comply with a collection of information if it does not display a currently valid OMB control number.
PLEASE DO NOT RETURN YOUR FORM TO THE ABOVE ADDRESS.

1. REPORT DATE (DD-MM-YYYY)	2. REPORT TYPE	3. DATES COVERED (From - To)
31-08-2010	Final Report	21-May-2007 - 20-May-2010

4. TITLE AND SUBTITLE

INFLUENCE OF ZWITTERIONS ON PROPERTIES AND MORPHOLOGY OF IONOMERS: IMPLICATIONS FOR ELECTRO-ACTIVE APPLICATIONS

5a. CONTRACT NUMBER

W911NF-07-1-0339

5b. GRANT NUMBER

5c. PROGRAM ELEMENT NUMBER

611102

6. AUTHORS

Tianyu Wu, Rebecca H. Brown, Andrew J. Duncan, Frederick L. Beyer, Timothy E. Long

5d. PROJECT NUMBER

5e. TASK NUMBER

5f. WORK UNIT NUMBER

7. PERFORMING ORGANIZATION NAMES AND ADDRESSES

Virginia Polytechnic Institute & State University
Office of Sponsored Programs
Virginia Polytechnic Institute and State University
Blacksburg, VA 24060 -

8. PERFORMING ORGANIZATION REPORT NUMBER

9. SPONSORING/MONITORING AGENCY NAME(S) AND ADDRESS(ES)

U.S. Army Research Office
P.O. Box 12211
Research Triangle Park, NC 27709-2211

10. SPONSOR/MONITOR'S ACRONYM(S)

ARO

11. SPONSOR/MONITOR'S REPORT NUMBER(S)

51466-CH.4

12. DISTRIBUTION AVAILIBILITY STATEMENT

Approved for Public Release; Distribution Unlimited

13. SUPPLEMENTARY NOTES

The views, opinions and/or findings contained in this report are those of the author(s) and should not contrued as an official Department of the Army position, policy or decision, unless so designated by other documentation.

14. ABSTRACT

The influence of tailored electrostatic interactions on the physical properties and morphology of high performance polymeric membranes remains as a critical concern for emerging technologies. We demonstrated earlier the synthesis of acrylic-based sulfobetaine-containing copolymers in non-fluorinated solvents, and the electrospinning of such copolymers below the expected entanglement concentration. Swelling of the zwitterionomer membranes in EMIm ES ionic liquid at 10 wt% IL concentration resulted in composites with similar mechanical performance, but

15. SUBJECT TERMS

zwitterionomer, thermal mechanical property, morphology, ionic liquid, ionic conductivity, transducer

16. SECURITY CLASSIFICATION OF:			17. LIMITATION OF ABSTRACT	15. NUMBER OF PAGES	19a. NAME OF RESPONSIBLE PERSON
a. REPORT	b. ABSTRACT	c. THIS PAGE			Timothy Long
UU	UU	UU	UU		19b. TELEPHONE NUMBER: 540-231-2480

Report Title

INFLUENCE OF ZWITTERIONS ON PROPERTIES AND MORPHOLOGY OF IONOMERS: IMPLICATIONS FOR ELECTRO-ACTIVE APPLICATIONS

ABSTRACT

The influence of tailored electrostatic interactions on the physical properties and morphology of high performance polymeric membranes remains as a critical concern for emerging technologies. We demonstrated earlier the synthesis of acrylic-based sulfobetaine-containing copolymers in non-fluorinated solvents, and the electrospinning of such copolymers below the expected entanglement concentration. Swelling of the zwitterionomer membranes in EMIm ES ionic liquid at 10 wt% IL concentration resulted in composites with similar mechanical performance, but significantly higher ionic conductivities. In this work, we designed cationic ionomers bearing methanesulfonate anions for a direct comparison to the sulfobetaine-containing copolymers. We determined, employing DMA, SAXS and AFM, that the zwitterionomer films have superior mechanical performance to their cationic analogs and are more microphase separated. We propose that the stronger electrostatic interactions with zwitterions are ionic in nature, different from the dipole-dipole interactions in typical ionomers. In an effort to prepare zwitterionomer-based electro-active devices, we prepared zwitterionomer/EMIm ES composites using both the "swelling" and the "cast with" methods. A correlation of DMA, SAXS, and impedance spectroscopy results revealed that the sample preparation methods had a profound influence of the mechanical and electrical performance of the composite membranes.

List of papers submitted or published that acknowledge ARO support during this reporting period. List the papers, including journal references, in the following categories:

(a) Papers published in peer-reviewed journals (N/A for none)

Brown, R.H.; Duncan, A.J.; Choi, J.H.; Park, J.K.; Wu, T.; Leo, D.J.; Winey, K.I.; Moore, R.B.; Long, T.E. Effect of Ionic Liquid on Mechanical Properties and Morphology of Zwitterionic Copolymer Membranes. Macromolecules. 2010, 43, 790-796.

Number of Papers published in peer-reviewed journals: 1.00

(b) Papers published in non-peer-reviewed journals or in conference proceedings (N/A for none)

Number of Papers published in non peer-reviewed journals: 0.00

(c) Presentations

Probing structure and thermal properties of ionic liquid-containing zwitterionomers at the nanoscale
Germinario, Louis T.; Sahagian, Khoren; Brown, Rebecca H.; Kjoller, Kevin; Wu, Tianyu; Long, Timothy E.
38th North American Thermal Analysis Society Annual Conference, Philadelphia, PA, United States, August 15-18, 2010, Abstract ID No.: 98

Number of Presentations: 1.00

Non Peer-Reviewed Conference Proceeding publications (other than abstracts):

Influence of zwitterions on properties and morphology of ionomers: implications for electro-active applications
Wu, Tianyu; Duncan, Andrew J.; Brown, Rebecca H.; Beyer, Frederick L.; Long, Timothy E.
Preprints, International Symposium on Polymer Chemistry (PC 2010), Suzhou, China P.R., June 2-6, 2010 (2010), 347-348.

Number of Non Peer-Reviewed Conference Proceeding publications (other than abstracts): 1

Peer-Reviewed Conference Proceeding publications (other than abstracts):

Number of Peer-Reviewed Conference Proceeding publications (other than abstracts): 0

(d) Manuscripts

N/A

Number of Manuscripts: 0.00

Patents Submitted

Patents Awarded

Graduate Students

NAME	PERCENT_SUPPORTED
Tianyu Wu	0.25
Shijing Cheng	0.25
FTE Equivalent:	**0.50**
Total Number:	**2**

Names of Post Doctorates

NAME	PERCENT_SUPPORTED
Eugene Joseph	0.15
FTE Equivalent:	**0.15**
Total Number:	**1**

Names of Faculty Supported

NAME	PERCENT_SUPPORTED
FTE Equivalent:	
Total Number:	

Names of Under Graduate students supported

NAME	PERCENT_SUPPORTED
FTE Equivalent:	
Total Number:	

Student Metrics

This section only applies to graduating undergraduates supported by this agreement in this reporting period

The number of undergraduates funded by this agreement who graduated during this period:	0.00
The number of undergraduates funded by this agreement who graduated during this period with a degree in science, mathematics, engineering, or technology fields:.....	0.00
The number of undergraduates funded by your agreement who graduated during this period and will continue to pursue a graduate or Ph.D. degree in science, mathematics, engineering, or technology fields:.....	0.00
Number of graduating undergraduates who achieved a 3.5 GPA to 4.0 (4.0 max scale):	0.00
Number of graduating undergraduates funded by a DoD funded Center of Excellence grant for Education, Research and Engineering:	0.00
The number of undergraduates funded by your agreement who graduated during this period and intend to work for the Department of Defense	0.00
The number of undergraduates funded by your agreement who graduated during this period and will receive scholarships or fellowships for further studies in science, mathematics, engineering or technology fields:	0.00

Names of Personnel receiving masters degrees

NAME

Total Number:

Names of personnel receiving PHDs

NAME

Total Number:

Names of other research staff

NAME PERCENT_SUPPORTED

FTE Equivalent:

Total Number:

Sub Contractors (DD882)

Inventions (DD882)

Scientific Progress and Accomplishments

Introduction

Ion-containing polymers and polyelectrolytes have attracted considerable scientific attention over the past 20 years.[1] They have shown unique physical properties that combine the electrical conductivity of low molar mass electrolytes and the viscoelastic characteristics of polymers. Such properties promise polymeric materials in emerging technologies including energy,[2] water purification,[3] and biotechnology[4] among others.

Zwitterions are charged species that contain equal numbers of cations and anitions. Typically, the cations are quaternary amines, while the anions vary among carboxylates, sulfonates, and phosphates. The corresponding zwitterions are referred to as carbobetaines, sulfobetaines and phosphobetaines respectively. The unique presence of opposite charges covalently linked in most cases through alkylene spacers offers extremely high polarities. Typical dipole moments of sulfobetaine-type zwitterions are reported as $\mu \sim 18.7\text{-}27.6$ Debye (D),[5] whereas that of water is only 1.9 D. Therefore, strong charge interactions are ubiquitous among zwitterions.

Polyzwitterions have received considerable scientific attention over the past thirty years. Kudaibergenov et al. recently reviewed synthesis, characterization and application of polymeric betaines.[6] A major interest in zwitterion-containing polymers involves the fact that betaines, phosphobetaines in particular, are synthetic analogs to phosphorylcholine in cell membranes. Jiang and coworkers have demonstrated ultralow fouling characteristics of polysulfobetaine grafted surfaces in marine environments.[7,8] Cheng et al. attributed such biocompatibility of polyzwitterions to their ability to form a dynamic boundary layer after hydration.[9] McCormick and coworkers focused on the controlled polymerization of zwitterion-containing polymers in

aqueous media via RAFT,[10] and demonstrated stimuli-responsiveness of polyzwitterions to pH and ionic strength in solutions.[11,12] Galin and coworkers studied extensively the solid state properties of ethyl acrylate and *n*-butyl acrylate (*n*BA) based sulfobetaine-containing polymers.[13,14] They demonstrated that the incorporation of zwitterionic functionalities affords elastomeric characteristics, typical of ionomers, to low T_g polymer matrices.[15-19] In a parallel effort, Gauthier et al. investigated the influence of the spacer length between the opposite charges and the bulkiness around the cations on the elastomeric performance of polyzwitterions.[20] They found that the influence of intercharge spacing was insignificant, while the bulkiness around cations hinders the binding between different sulfobetaine units.

Polymeric betaines have also exhibited remarkable miscibility with various inorganic and metallic salts up to stoichiometric quantities.[21-23] These salt-polyzwitterion mixtures formed amorphous blends due to strong ion-dipole interactions that precluded salt segregation or crystallization within the zwitterion matrix. This unique ability to dissolve large amounts of salts have sparked interest in polyzwitterions as polymeric host matrices for polar guest molecules.[23]

Ionic liquids (ILs) have become increasingly important in recent years for applications spanning many fields of chemistry. ILs are molten salts that are liquids below 100 °C and exhibit excellent properties including chemical and thermal stability, low vapor pressure, and high ionic conductivity.[24] Although widely used as solvents for synthesis and extractions, ILs are also used as diluents in polymer membranes to afford high conductivities for applications including lithium batteries,[25-27] solar cells,[24,28-30] and electromechanical transducers.[31-34] For example, replacing water with an IL as the diluent in Nafion™ membranes for ionic polymer transducers resulted in an increase from 30,000 cycles to more than 250,000 cycles.[35] This

drastic change was due to a lack of solvent evaporation for ILs, which lead to deterioration of transducer performance after 30,000 cycles with water as the diluent.

The goal of our ARO sponsored single investigator award is to first investigate the influence of tethered counterions on the physical properties, as well as the morphology, of ionomers. We synthesized 2-(*n*-butyldimethylamino)ethyl 2-methacrylate methanesulfonate (BDMAEMA MS), as shown in **Scheme 1**, the cationic analog of 3-[[2-(methacryloyloxy)ethyl](dimethyl)ammonio]-1-propanesulfonate (SBMA). Through copolymerizing the two charge-containing monomers with *n*BA, a series of zwitterionomers and their corresponding cationic analogs were synthesized. The thermal stability, glass transition temperatures and thermal mechanical behavior of the copolymers were probed using thermogravimetric analysis (TGA), differential scanning calorimetry (DSC), and dynamic mechanical analysis (DMA) respectively. The morphological differences between the two copolymer series were studied using small angle X-ray scattering (SAXS) and atomic force microscopy (AFM) imaging. Through a correlation between the elastomeric performances of the copolymers and their morphologies, we aim to elucidate the molecular difference between zwitterionic interaction and typical ionic interactions. Such fundamental understanding will provide us with guidance in the design of charge-containing polymer for advanced applications.

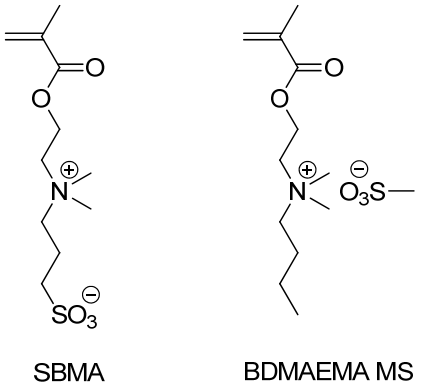

SBMA BDMAEMA MS

Scheme 1 Charge-Containing Monomers: Analogs to Probe Influence of Mobile Anions.

Secondly, we explored the interaction of ionic liquids with low T_g ionomers featuring moderate loadings of dipolar sulfobetaine-based zwitterions. We introduced the ionic liquids into the polymer matrices via both the "swelling" and the "cast with" methods. ILs are expected to interact with the zwitterion functionality in a similar fashion to inorganic salts or polar liquids (water, glycerol, ethylammonium nitrate) previously reported.[36] However, the difference in the distribution of the IL in the polymer membranes should have an influence on the mechanical and the electrochemical performance of the sample. We employed DMA, SAXS, and impedance spectroscopy to study the partitioning of IL within the zwitterionic membrane, as well as its effects on polymer morphology. Incorporation of ILs with high ionic conductivities into zwitterion-containing copolymers may have implications in the use of zwitterionomer membranes in electronic devices, where the lack of mobile counterions in the membrane serves as a fundamental difference from current ionomers.

Experimental

Materials

Zwitterionic monomer, 3-[[2-(methacryloyloxy)ethyl](dimethyl)ammonio]-1-propanesulfonate (SBMA), was graciously provided by Raschig GmbH. *n*-Butyl acrylate (*n*BA), dimethyl sulfoxide (DMSO, 99.9+%) and hydroquinone (99%) were purchased from Alfa Aesar. 2-(Dimethylamino)ethyl methacrylate (DMAEMA), 1-bromobutane, silver methanesulfonate (AgMS), azobisisobutyronitrile (AIBN) and 1-ethyl-3-methylimidazolium ethylsulfate (EMIm ES) were acquired from Sigma-Aldrich. Diethyl ether (anhydrous) was bought from Mallinckrodt. Chloroform (Optima grade), methylene chloride and methanol (HPLC grade) were purchased from Fisher Scientific. AIBN was recrystallized from methanol. DMAEMA and *n*BA were passed through neutral alumina columns, and *n*BA was further distilled under reduced pressure from calcium hydride. DMSO and EMIm ES were stored over molecular sieves (3A). Ultrapure water having a resistivity of 18.2MΩ·cm was obtained using a Millipore Direct-Q5 purification system. All other chemicals were used as received.

Synthesis of 2-(*N*-butyl-*N*,*N*-dimethylamino)ethyl methacrylate methanesulfonate (BDMAEMA MS)

The synthesis of BDMAEMA MS is illustrated in **Scheme 1**. DMAEMA (30.0 g, 0.191 mol), 1-bromobutane (52.3 g, 0.388 mol), methylene chloride (40 mL, 35 vol%) and hydroquinone (6.0 g) were added to a 250-mL, round-bottomed flask with a magnetic stir bar. The reaction mixture was sparged with N_2 for 15 min and placed into an oil bath at 50 °C for 72 h. The product, 2-(*N*-butyl-*N*,*N*-dimethylamino)ethyl methacrylate bromide (BDMAEMA Br),

was precipitated into and washed with diethyl ether (anhydrous), recrystallized from acetone and dried under vacuum at room temperature. A yield of 70% was obtained.

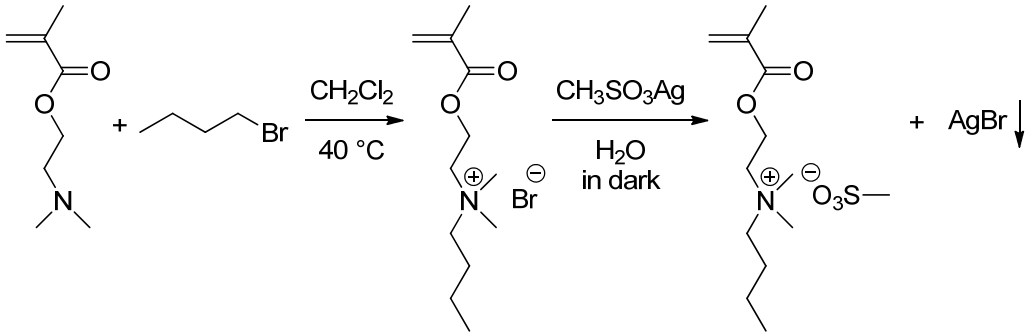

Scheme 1. Synthesis of BDMAEMA Br in the presence of free radical inhibitor (hydroquinone) and subsequent anion exchange to BDMAEMA MS

Anion exchange of BDMAEMA Br was then conducted at room temperature. AgMS (1.00 g, 4.92 mmol) and BDMAEMA Br (1.45 g, 4.93 mmol) were dissolved in 15 mL and 5 mL Milli-Q water respectively in 20-mL scintillation vials. After full dissolution, the AgMS solution was transferred to a 120-mL amber container and the BDMAEMA Br solution was subsequently added in the absence of light. Both vials were thoroughly rinsed with Milli-Q water after solution transfer. The reaction was allowed to equilibrate in the dark overnight, though the precipitation of AgBr was instantaneous. The BDMAEMA MS solution was finally filtered through a fine fritted funnel and lyophilized dry. A yield of 97% was obtained. ^{1}H NMR (400 MHz, D_2O, δ): 1.03 (t, 3H, -$CH_2CH_2CH_2CH_3$), 1.45 (m, 2H, -$CH_2CH_2CH_2CH_3$), 1.85 (m, 2H, -$CH_2CH_2CH_2CH_3$), 2.02 (s, 3H, =C(CO)CH_3), 2.88 (s, 3H, $^{-}OS(=O)_2CH_3$), 3,24 (s, 6H, -$CH_2N(CH_3)_2CH_2$-), 3.46 (m, 2H, -$OCH_2CH_2N(CH_3)_2CH_2$-), 3.84 (m, 2H, -$OCH_2CH_2N(CH_3)_2CH_2$-), 4.73 (m, 2H, -$OCH_2CH_2N(CH_3)_2CH_2$-), 6.05 (d, J = 75.8 Hz, 2H, C=CH_2).

Synthesis of poly(*n*BA-*co*-SBMA) and poly(*n*BA-*co*-BDMAEMA MS)

The syntheses of poly(*n*BA-*co*-SBMA) are illustrated in **Scheme 2**. A typical copolymerization of poly(*n*BA-*co*-SBMA) containing 10 mol% SBMA is described as follows: *n*BA (5.00 g, 390 mmol), SBMA (1.21 g, 4.33 mmol) and AIBN (31.1 mg) were charged to a 150-mL round-bottomed flask with a magnetic stir bar. DMSO (51.1 mL, 90 wt%) was added to dissolve the monomers. The reaction mixture was sparged with N_2 for 15 min, and placed into an oil bath at 65 °C for 24 h. The polymer was precipitated into water, and allowed to equilibrate in ultrapure water for a week. A yield of 90% was obtained. The final product was monomer free, as confirmed via ^{1}H NMR, and any residual DMSO was removed under vacuum at 65 °C for 3 days.

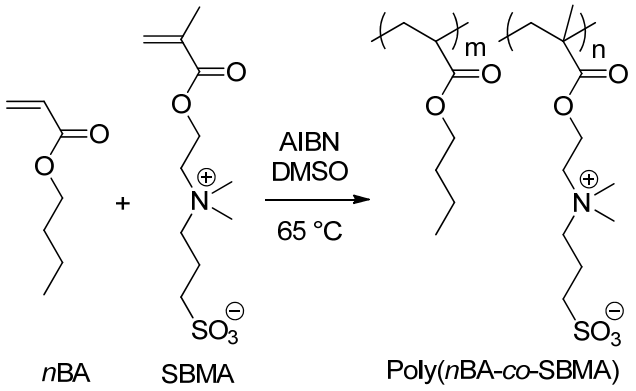

Scheme 2. Synthesis of Poly(*n*BA-*co*-SBMA) using conventional free radical polymerization

The syntheses of poly(*n*BA-*co*-BDMAEMA MS) were conducted under similar conditions with 10 wt% monomers in the reaction mixtures and 0.5 wt% AIBN based on total monomers. However, due to very different solubility, poly(*n*BA-*co*-BDMAEMA MS) were first isolated via vacuum stripping of DMSO. The products were then dissolved in methanol and diluted with ultrapure water. The product solutions remained homogeneous upon H_2O addition and after rotavap removal of methanol. Further purification of the copolymers was performed via

exhaustive dialysis. ^{1}H NMR spectra also confirmed that monomer residue was not present in the final products. Typical yields of 85% were achieved.

Membrane Preparation and Ionic Liquid Incorporation

Neat films were solution cast from either chloroform (for poly(*n*BA-*co*-SBMA)) or methanol (for poly(*n*BA-*co*-BDMAEMA MS)) at 0.1 g/mL concentration into Teflon® molds. Films were first dried at room temperature overnight, then placed into vacuum oven at 65 °C for 72 h, and finally kept in vacuum at room temperature until use.

Ionic liquid, EMIm ES, incorporation into poly(*n*BA-*co*-SBMA) were achieved via two different methods: the "swelling" method and the "cast with" method. In the "swelling" approach, dry films were immersed in EMIm ES, and stored in sealed glass jars inside a vacuum oven at 65 °C. Swollen samples were periodically weighed to determine the uptake of IL. Specifically, films were handled using forceps and blotted with a Kimwipe® to remove excess EMIm ES on the polymer surface. IL uptake was calculated according to the following equation:

$$wt\%\ uptake = \frac{m - m_0}{m_0}$$

where m_o is the initial dry film mass and m is the mass of the swollen film at a given time.

Alternatively, in the "cast with" approach, poly(*n*BA-*co*-SBMA) and EMIm ES were premixed in chloroform. The film casting and drying processes were the same as those described above for the neat films. The IL contents in the "cast with" films were calculated according to the following equation:

$$wt\%\ of\ IL = \frac{m_{IL}}{m_p}$$

where m_{IL} is mass of the IL and m_p is the mass of the polymer.

All films were cut into strips approximately 20 mm x 5 mm for dynamic mechanical analysis and 8 mm diameter circles for electrical impedance spectroscopic analysis.

Instrumentation

1H NMR spectra were obtained on a Varian Unity 400 Mz spectrometer in D_2O, $CDCl_3$ and CD_3OD. Dynamic Light Scattering (DLS) measurements were performed on a Malvern Zeta Sizer nano Series Nano ZS instrument at a wavelength of 633 nm and a scattering angle of 173°. The experiments were performed at a temperature of 25 °C. Polymer samples were prepared at 1 mg/mL concentration and were syringed through 0.2 μm PTFE filters directly into clean cuvettes. DLS data were observed for the presence or absence of aggregation peaks based on particle diameter size. Size exclusion chromatography (SEC) was used to determine the molecular weights of the copolymers at 50 °C in DMF with 0.01 M LiBr at 1 mL min^{-1} flow rate. The DMF SEC system was equipped with a Waters 717plus autosampler, a Waters 1525 HPLC pump, two Waters Styragel HR5E (DMF) columns, and a Waters 2414 differential refractive index detector. Relative molecular weights to polystyrene standards are reported.

Thermogravimetric analysis (TGA) of the samples were conducted with a TA Q500 from room temperature to 700 °C at a heating rate of 10 °C·min^{-1} under N_2 atmosphere. Differential scanning calorimetry (DSC) measurements were made on a TA Q100 instrument at a heating and cooling rate of 10 °C/min from -90 °C. The first heat scans were stopped at 120 °C, and the traces of the second heats are reported. Dynamic mechanical analysis (DMA) was performed on a TA Q800 analyzer in tension mode, at 1 Hz frequency, 15 μm amplitude, and 3 °C/min heating rate from -90 °C.

A Veeco MultiMode scanning probe microscope was used with Veeco's MPP-21100-10 tips, having spring constants of 3 N/m, for tapping-mode AFM imaging. Samples were imaged at a set-point to free-air amplitude ratio of 0.6 and at magnifications of 600 nm ×600 nm.

Small angle X-ray scattering data were collected with a customized pinhole collimated 3 m camera. X-rays were generated with a Rigaku Ultrax18 rotating Cu anode generator operated at 45 kV and 100 mA and then filtered with Ni foil to select the Cu K_α doublet (λ = 1.542 Å). Two-dimensional data sets were collected using a Molecular Metrology multiwire area detector, located at about 150 cm from the sample. The raw data were corrected for absorption and background noise and then azimuthally averaged. The corrected data were placed on an absolute scale using a sample of type 2 glassy carbon previously calibrated at the Advance Photon Source, Argonne National Laboratory. All data reduction and analysis were performed using Igor Pro v6.12A from Wavemetrics, Inc.

Electrical impedance spectroscopy (EIS) was performed with a Solartron Impedance analyzer from 1 MHz to 0.1 Hz. The instrument was operated in potentiostatic mode to apply a single 100 mV rms sine wave while measuring the complex impedance response of the sample. A custom fixture aligned two parallel circular brass plates of 0.327 cm diameter to allow for thru-plane impedance measurements. Ionic conductivity values (σ, mS/cm) were calculated using the following equation:

$$\sigma = \frac{4 \cdot t}{\pi \cdot d^2 \cdot R}$$

where R is the bulk membrane resistance (Ohms), t (cm) is the sample thickness, and d (cm) is the electrode diameter, which is always smaller than the sample diameter. The kinetic portion of the complex impedance data (Nyquist plot) was fit with a semicircle to extrapolate the membrane resistance as the low frequency x-intercept where the imaginary impedance equals zero.

Results and Discussions

Synthesis and Characterization of BDMAEMA MS

BDMAEMA MS was synthesized via quaternization of DMAEMA with 1-bromobutane and subsequent anion exchange with equimolar of AgMS. The structure of this novel monomer was confirmed via ^{1}H NMR spectroscopy (**Figure 1**), ^{13}C NMR spectroscopy (**Figure 2**) and elemental analysis (**Table 1**). A melting point was observed in the first heat of the DSC at 160 °C.

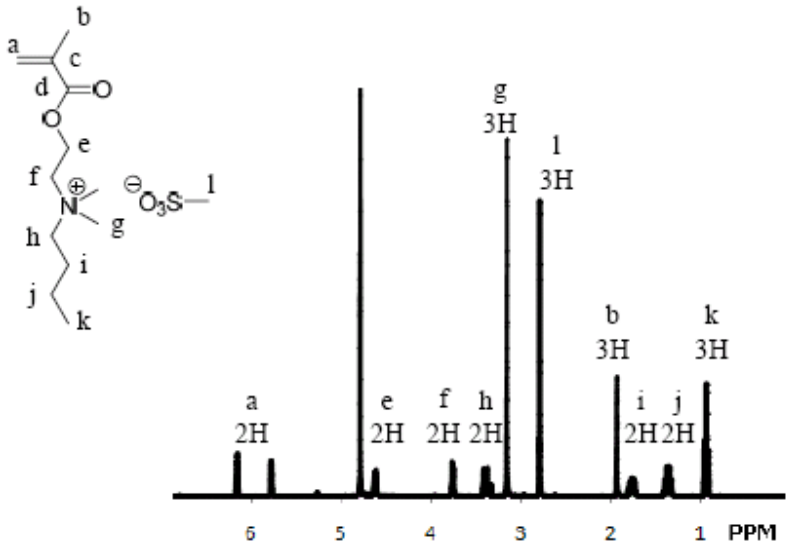

Figure 1. ^{1}H NMR of BDMAEMA MS in D_2O

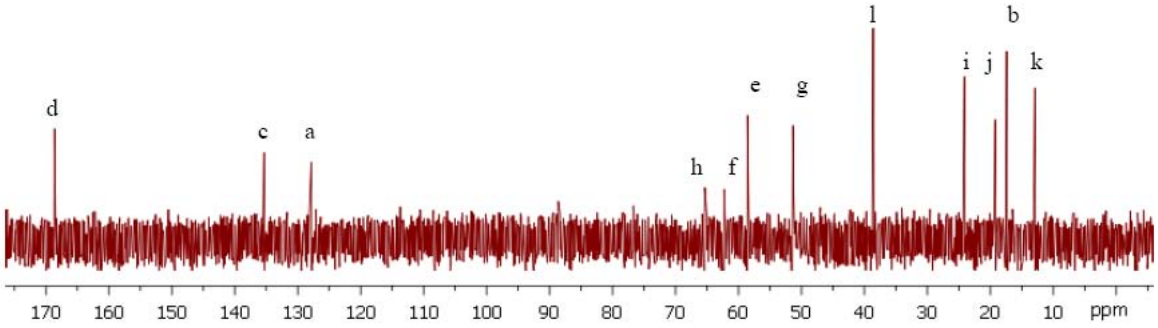

Figure 2. ^{13}C NMR of BDMAEMA MS in D_2O

Quaternized DMAEMAs that bear a butyl tail and various halide anions, such as Cl, Br and I, or PF_6 anion have been reported in the literature.[37-40] Here, we designed novel BDMAEMA MS to serve as the cationic analog to SBMA, which also contains quaternary ammonium cation and an organic sulfonate anion. The butyl tail in BDMAEMA MS was chosen to match the size of the cationic analog to that of SBMA. The new monomer allowed us to conduct direct comparison between the zwitterionic functionality and its cationic analog.

Table 1. Elemental analysis results of BDMAEMA MS

Element	Theory (wt%)	Found (wt%)
C	50.46	50.49
H	8.80	8.79
O	25.85	26.03
N	4.53	4.49
S	10.36	10.33

Synthesis and Structural Characterization of Poly(*n*BA-*co*-SBMA) and Poly(*n*BA-*co*-BDMAEMA MS)

Zwitterionic copolymers containing 3, 6, and 9 mol% SBMA were synthesized using conventional free radical copolymerization in DMSO. The reactions were allowed to reach high conversions in 24 h. ^{1}H NMR spectra, as shown in **Figure 3**, confirmed that the products were monomer-free. Peak ‘a’ at 0.95 ppm is assigned to the methyl group on *n*BA, while peak ‘b’ at 3.36 ppm is assigned to the two methyl groups on the quaternized “N” of SBMA. The amount of SBMA in the copolymer was determined using the following equation:

$$SBMA\ mol\% = \frac{100b}{b + 2a}\%$$

and the copolymer compositions matched the feeds within 1 mol%.

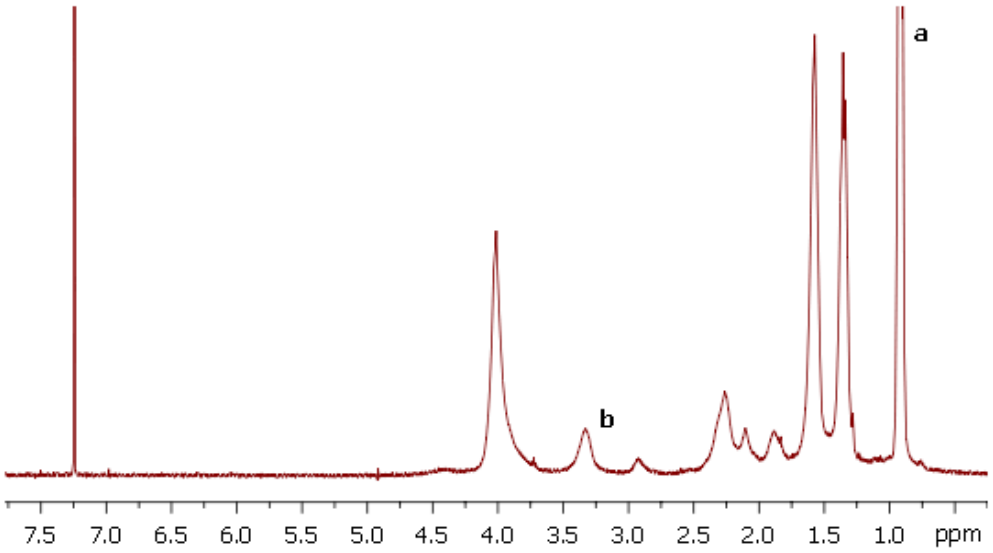

Figure 3. ^{1}H NMR of poly(*n*BA-*co*-SBMA) in $CDCl_3$

The cationic analogs containing 7, 10, 15 and 22 mol% BDMAEMA $MeSO_3$ were synthesized under similar conditions to those for the zwitterionomers. However, the product isolation step was quite different due to the very different solubility between the zwitterionomers and their cationic analogs. Nevertheless, the absence of the monomers in the final products was also confirmed via ^{1}H NMR spectra, as shown in **Figure 4**. Peak 'c' at 0.97 ppm is assigned to the methyl group on *n*BA, while peak 'd' at 1.05 ppm and the shoulder "e' on its left are assigned to the two methyl groups on BDMAEMA MS. The copolymer compositions were determined using the following equation:

$$BDMAEMA\ MS\ mol\% = \frac{100(d+e)}{2c+d+e}\%$$

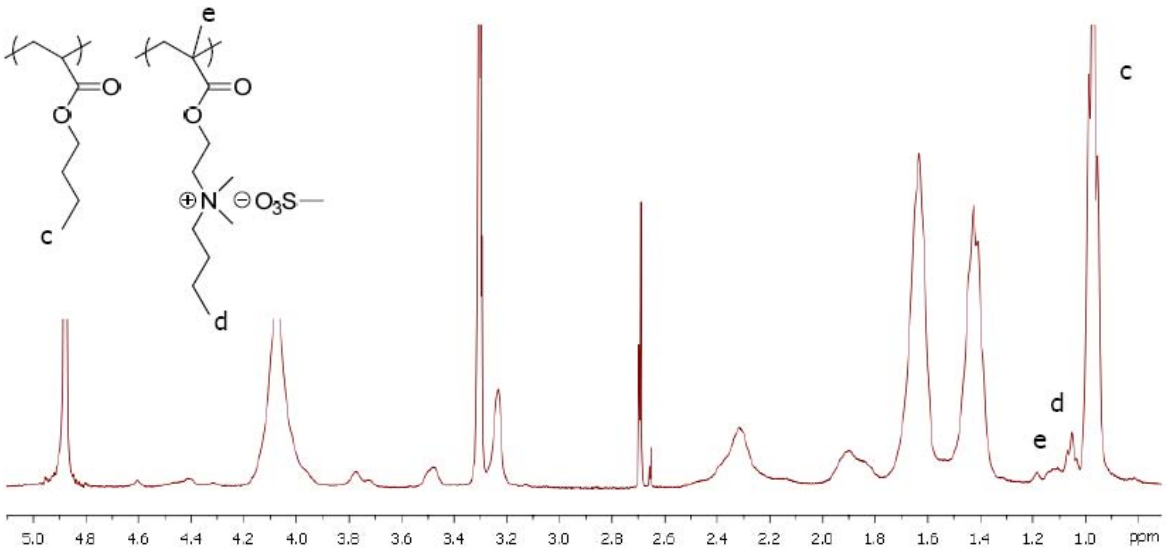

Figure 4. ^{1}H NMR of poly(*n*BA-*co*-BDMAEMA MS) in CD_3OD

The characterization of the molecular weights of charge-containing polymers using size exclusion chromatography presents a challenge due to ionic association of the polymers in solution. Layman et al. demonstrated the use of dynamic light scattering technique in the screening of suitable SEC solvents for water-soluble ionenes.[41] Here, we adopted the same methodology, and determined that DMF with 0.01 M LiBr is a suitable SEC eluent for both poly(*n*BA-*co*-SBMA) and poly(*n*BA-*co*-BDMAEMA MS) . **Figure 5** is a representative DLS trace of poly(nBA$_{91}$-*co*-SBMA$_9$) in DMF with 0.01 M LiBr.

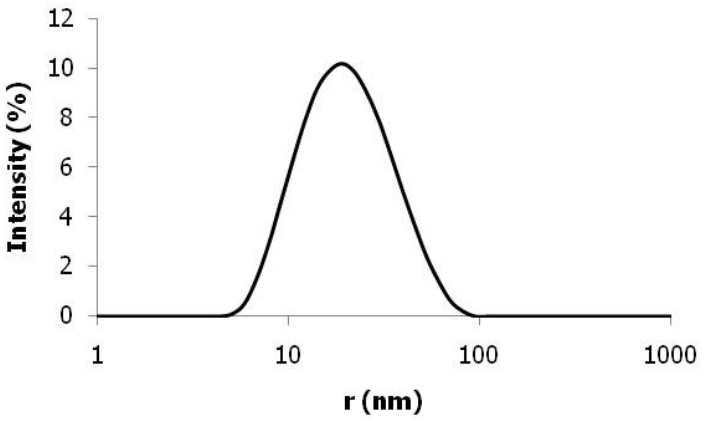

Figure 5. DLS intensity *vs* radius plot of poly(nBA$_{91}$-*co*-SBMA$_9$) in DMF with 0.01 M LiBr

The single peak with an average diameter of 22.7 nm suggests that the polymer is not aggregating in solution. SEC reproducibility tests also confirm that the selected SEC condition is suitable for both copolymer systems, except the cationic analog containing a high 22 mol% BDMAEMA MS. We attribute the irreproducibility of this sample to the interaction between the polymer and the column at high BDMAEMA MS compositions. **Table 2** lists the relative molecular weights of the other copolymers to polystyrene (PS) standards.

Table 2. Size exclusion chromatographic analysis of the copolymers

Copolymer Composition	M_n (kg/mol)	M_w (kg/mol)	PDI
poly(nBA$_{97}$-*co*-SBMA$_3$)	70.8	384	5.43
poly(nBA$_{94}$-*co*-SBMA$_6$)	94.5	405	4.30
poly(nBA$_{91}$-*co*-SBMA$_9$)	69.8	274	3.92
poly[nBA$_{93}$-co-BDMAEMA MS$_7$]	68.0	281	4.13
poly[nBA$_{90}$-co-BDMAEMA MS$_{10}$]	47.8	181	3.78
poly[nBA$_{87}$-co-BDMAEMA MS$_{15}$]	9.30	24.7	2.32

Thermal Characterization of Zwitterionomers and their Cationic Analogs

The thermal stability of the copolymers was determined using thermogravimetric analysis. **Figure 6** shows the representative TGA traces of copolymers containing 9 mol% SBMA and 10 mol% BDMAEMA MS. The 5% weight loss temperatures of poly(*n*BA-*co*-SBMA) was 299 °C, similar to poly(*n*BA-*co*-BDMAEMA MS) at 292 °C. Burch and Manring showed that the thermal degradation of similar quaternary ammonium-containing polymers follows the Hofmann elimination mechanism.[42] Since the MS anion in BDMAEMA MS has similar basicity to the sulfonate group in SBMA, it was expected that the copolymer containing 9 mol% SBMA had similar 5% weight loss temperature to its cationic analog. However, this finding may also suggest that the higher mobility of the MS anion in BDMAEMA MS does not

enable more access to the β-H of the quaternary ammonium than the covalently tethered sulfonate group in SBMA.

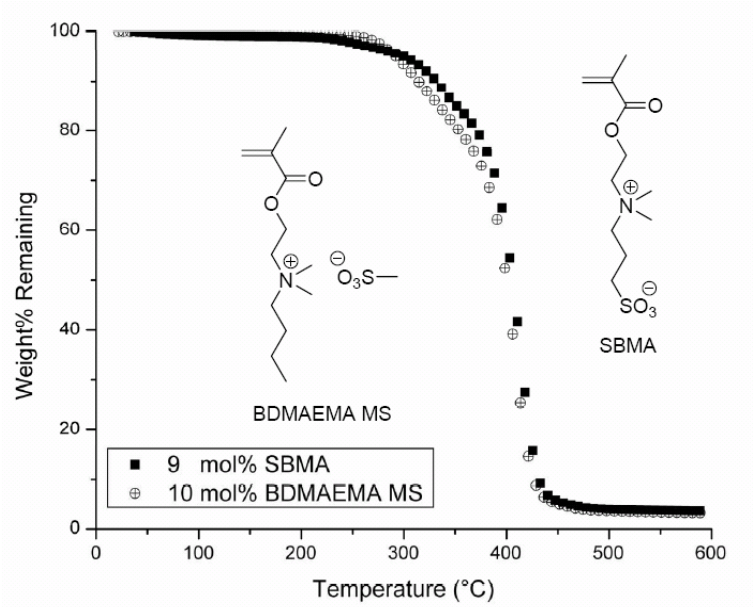

Figure 6. TGA of poly(*n*BA-*co*-SBMA) and poly(*n*BA-*co*-DBMAEMA MS) containing ~ 10 mol% of charged units

The glass transition temperatures of the copolymers were determined using differential scanning calorimetry, and the results are listed in **Table 3**. Only one glass transition temperature was observed for all copolymers. However, the glass transition temperatures for the zwitterionomers increased only slightly from -47 °C for poly(*n*BA) to -40 °C for copolymer containing 9 mol% SBMA. In comparison, the T_g of the cationic analog containing 7 mol% BDMAEMA MS was -35 °C, higher than the 9 mol% zwitterionomer. Further increase in the charged contents for the cationic analog to 15 mol% resulted in a glass transition temperature of -5 °C. Since the glass transition temperatures of poly(SBMA) and poly(BDMAEMA MS) homopolymers are 130 °C and 83 °C respectively, the different trends of T_g increase with increasing charge contents suggested that the zwitterionomers would exhibit a more phase-separated morphology than their cationic analogs.

Table 3. Glass transition temperatures of zwitterionomers and their cationic analogs

Copolymer Composition	T_g (°C)
poly(nBA)	-47
poly(nBA$_{97}$-*co*-SBMA$_3$)	-44
poly(nBA$_{94}$-*co*-SBMA$_6$)	-42
poly(nBA$_{91}$-*co*-SBMA$_9$)	-40
poly(SBMA)	130
poly[nBA$_{93}$-co-(BDMAEMA MS)$_7$]	-35
poly[nBA$_{90}$-co-(BDMAEMA MS)$_{10}$]	-26
poly[nBA$_{85}$-co-(BDMAEMA MS)$_{15}$]	-5
poly[nBA$_{78}$-co-(BDMAEMA MS)$_{22}$]	19
poly(BDMAEMA MS)	83

Mechanical Characterization of Zwitterionomers and Their Cationic Analogs

The thermal mechanical behaviors of the neat copolymers were characterized using dynamic mechanical analysis. **Figure 7** shows the overlaying DMA traces of the zwitterionomers and their cationic analogs. In agreement with the DSC results, the glass transitions for both 6 and 9 mol% zwitterionomers appeared near the same temperature, while those for the cationic analogs increased steadily with increasing charge contents in the copolymers. As expected, due to the dynamic nature of the DMA technique, the glass transitions temperatures of the samples measured using DMA are higher than those measured using DSC. More importantly, rubbery plateaus were observed only for the zwitterionomers, but not for the cationic analogs. We attribute these rubbery plateaus of the zwitterionomers to the physical cross-linking between zwitterionic functionalities.

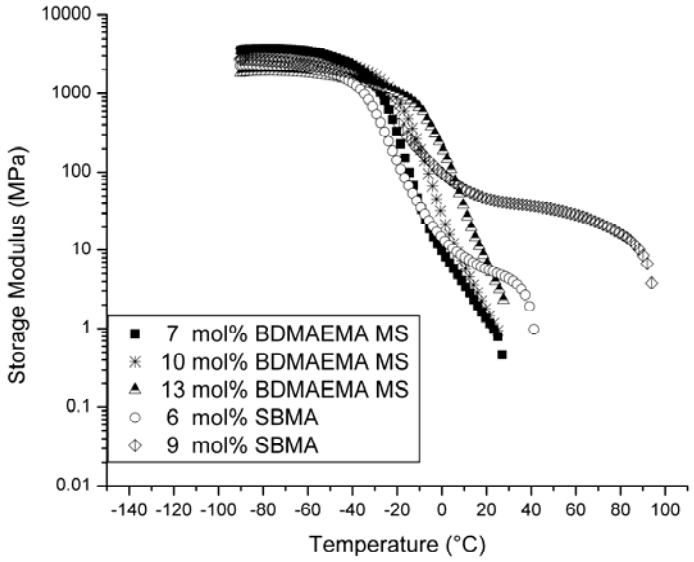

Figure 7. Storage modulus *vs* temperature profiles for poly(*n*BA-*co*-SBMA) and poly(*n*BA-*co*-BDMAEMA MS) containing varying amounts of charged units

Figure 8 illustrates proposed arrangements of the charged functionalities in the zwitterionomers and their cationic analogs. In a zwitterionomer, the quaternary ammonium cation and the sulfonate anion from one sulfobetaine functionality binds to another sulfobetaine in a head-to-tail fashion. Such binding interactions are ionic in nature, and may be strong enough to serve as physical crosslinks if the two sulfobetaine units are from different polymer backbones. However, in the case of the cationic analogs, due to the lack of covalent binding between the cations and the anions, the aggregation between two charged units should be driven by dipole-dipole interactions. Since dipole-dipole interactions are much weaker than ionic interactions, evidence of physical crosslinking was not observed for the cationic analogs in DMA.

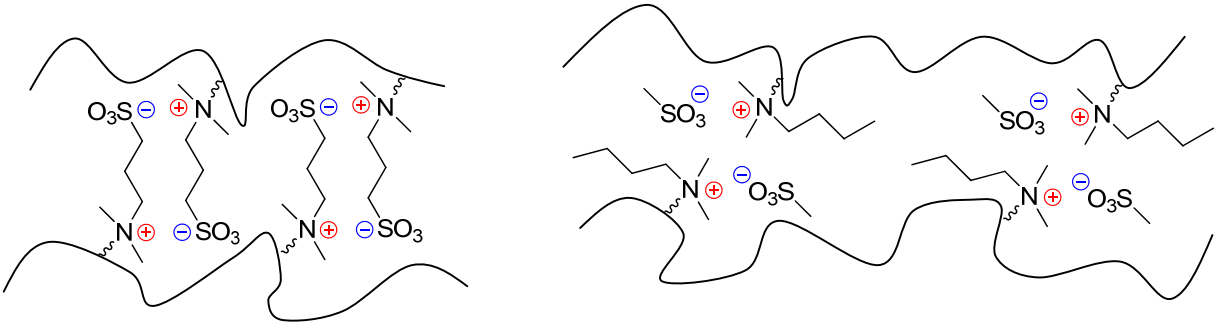

Figure 8. Illustration of the possible charge interactions in the zwitterionomers and their cationic analogs

Morphologies of Zwitterionomers and Their Cationic Analogs

The morphologies of the copolymers were probed in collaboration with Rick Beyer at ARL using small angle X-ray scattering (SAXS). Scattering profiles of the zwitterionomers and their cationic analogs, plotted as intensity *vs* scattering vector q on a log-linear plot, are shown in **Figure 9**.

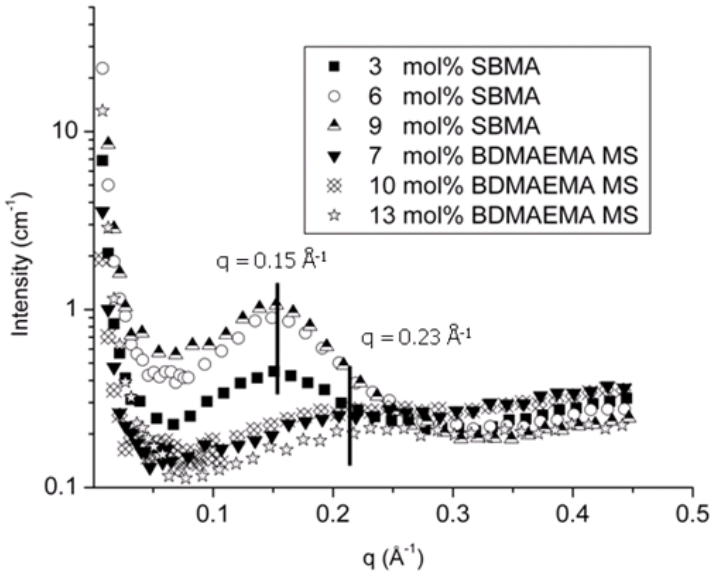

Figure 9. SAXS intensity *vs* scattering vector (q) traces for poly(*n*BA-*co*-SBMA) and poly(*n*BA-*co*-BDMAEMA MS) containing varying amounts of charged units

A scattering peak around q of 0.15 $Å^{-1}$ was observed for each of the zwitterionomer samples, and the scattering intensities decrease with decreasing sulfobetaine contents in the copolymers. Such scattering profiles are characteristic of charge-containing polymers, and the peaks are due to the different electron density between the ionic aggregates and the surrounding matrix. In comparison, the scattering peaks of the cationic analogs are much less distinctive, and have maxima around q of 0.20 $Å^{-1}$. This suggests that the cationic analog samples are less phase-separated than the zwitterionomers, in agreement with the DSC findings. The ionomer peak positions as a function of copolymer contents and the corresponding *d* spacings, calculated using the following equation, are summarized in **Table 4**.

$$d = \frac{2\pi}{q}$$

Table 4. Summary of scattering peaks and *d*-spacing for zwitterionomers and their cationic analogs

Copolymer Composition	Ionomer Peak	
	Position ($Å^{-1}$)	*d* spacing (Å)
poly(nBA$_{91}$-*co*-SBMA$_9$)	0.150	41.9
poly(nBA$_{94}$-*co*-SBMA$_6$)	0.153	41.1
poly(nBA$_{97}$-*co*-SBMA$_3$)	0.156	40.3
poly[nBA$_{87}$-co-(BDMAEMA MS)$_{15}$]	0.240	26.2
poly[nBA$_{90}$-co-(BDMAEMA MS)$_{10}$]	0.220	28.6
poly[nBA$_{93}$-co-(BDMAEMA MS)$_7$]	0.220	28.6

Atomic force microscopy technique was also employed to probe the morphologies of the zwitterionomers and their cationic analogs. The results are shown in **Figure 10**. For the zwitterionomers, clear evidence of phase separation was observed at very low zwitterion incorporation of 3 mol%. In comparison, the surface of the cationic analog that contains 10

mol% BDMAEMA MS looks very smooth; despite 22 mol% of charge, the cationic analog appears less phase-separated than the 3 mol% zwitterionomer. Such trend is in agreement with the SAXS findings. However, the dimensions of the AFM features are much larger than those determined using SAXS. Since AFM reveals surface morphology and SAXS analyzes bulk morphology, it is presumed that the samples have different surface and bulk morphologies. Another possible explanation for such discrepancy is that AFM offers lower resolution than SAXS. Nevertheless, the AFM results do confirm that the cationic analogs are less phase-separated than the zwitterionomers.

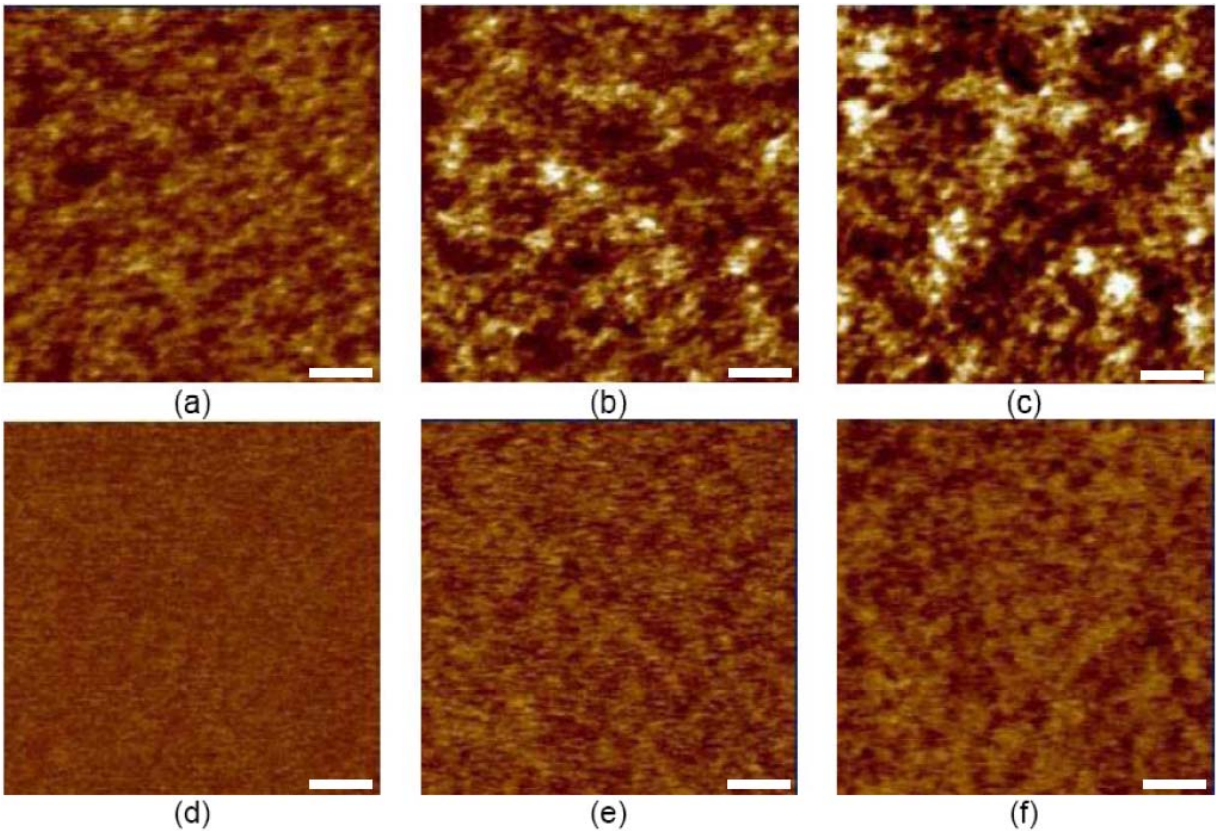

Figure 10. AFM images of zwitterionomers and their cationic analogs: samples (a~c) contains 3, 6 and 9 mol% SBMA respectively; samples (d~f) contains 10, 15 and 22 mol% BDMAEMA MS respectively. The scale bars represent 100 nm.

Introducing Ionic Liquid into Zwitterionomer Films

While the affinity of polybetaines for water and inorganic salts are well documented, their interactions with ionic liquids (IL) have received little attention.[43] In our earlier ARO-sponsored studies, we introduced 1-ethyl-3-methylimidazolium ethylsulfate (EMIm ES), an ionic liquid, into poly(*n*BA_{91}-*co*-$SBMA_9$) films via swelling, and studied its influence on the thermal mechanical performance and ionic conductivity of the zwitterionomer films.[44] We found that the zwitterionomer films were able to maintain their mechanical strength with up to 10 wt% EMIm ES incorporation, while their ionic conductivity increased with increasing IL contents in the membranes. The structure of EMIm ES is shown in **Figure 11**. It is a water-miscible IL with a melting point of -65 °C and bulk conductivity (σ) of 3.82 $mS \cdot cm^{-1}$ at 298K.

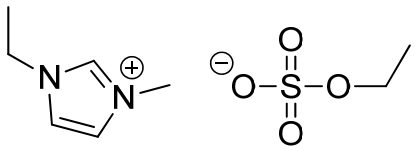

Figure 11. Structure of 1-ethyl-3-methylimidazolium ethylsulfate (EMIm ES).

There are two general approaches to incorporate ionic liquids into polymer membranes: the "swelling" approach and the "cast with" approach. Here, we focus on the influence of different ionic liquid incorporation methods on the properties of zwitterionomer/IL composite membranes. **Figure 12** illustrates the possible scenarios of ionic liquid distribution in the zwitterionomer membranes. We suppose that the "swollen" films should have a gradient distribution of the ionic liquid through the membrane, while the "cast with" films should afford a more homogeneous IL distribution. In order to further investigate the difference between the two sample preparation methods, we prepared both "swollen" and "cast with" samples with poly(*n*BA_{93}-*co*-$SBMA_7$) and EMIm ES, and conducted DMA and electrical impedance analysis

on the zwitterionomer/IL composites. The compositions of the samples studied are listed in **Table 5**.

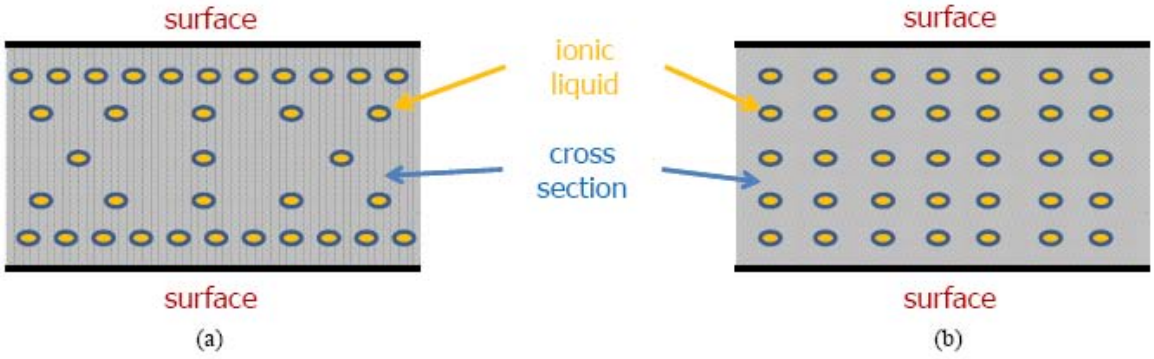

Figure 12. Proposed illustration of the distribution of ionic liquids in zwitterionomer membranes prepared via: (a) the "swolling" method and (b) the "cast with" method.

Table 5. List of poly(*n*BA_{93}-*co*-$SBMA_7$)/EMIm ES composite membranes prepared via "swollen" and "cast with" methods

Poly(*n*BA_{93}-*co*-$SBMA_7$)	"Swollen"	"Cast With"
wt% of EMIm ES	4.4	
	7.7	7.5
	8.8	
	11.2	11.2
	13.3	14.7
		17.3
		19.5

Mechanical Characterization of Zwitterionomer/IL Composite Membranes

The DMA traces of EMIm ES swollen poly(*n*BA_{93}-*co*-$SBMA_7$) are shown in **Figure 13**. The results agree with our previous literature stating that the zwitterionomer could maintains its mechanical strength with up to 10 wt% EMIm ES incorporation.[44] In fact, the data traces for 11.2

wt% and 13.3 wt% samples in the current study fall nicely into the transition region between 10.4 wt% and 19.7 wt% of the previous study, where the 19.7 wt% sample loses its mechanical strength at temperatures higher than its glass transition temperature.

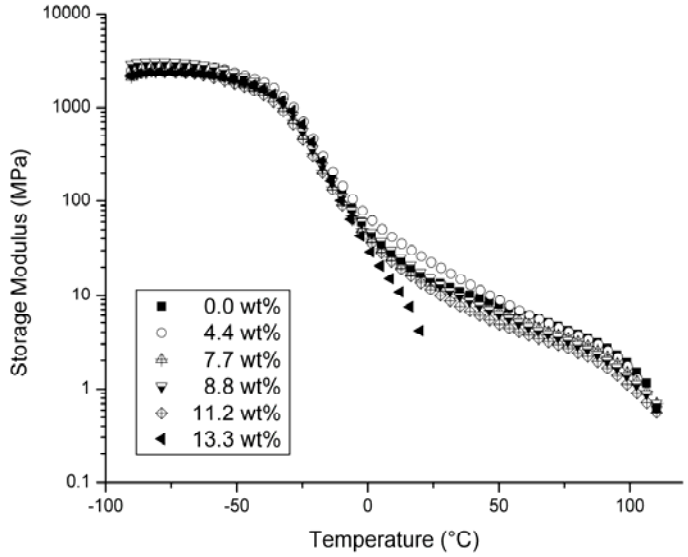

Figure 13. DMA traces of EMIm ES swollen poly(*n*BA_{93}-*co*-$SBMA_7$)

Figure 14 is the overlaying DMA traces of poly(*n*BA_{93}-*co*-$SBMA_7$) films cast with EMIm ES. Different from the "swollen" films, the "cast with" samples have shortened rubbery plateaus, an indication of weakened mechanical strength, upon ionic liquid incorporation. At 7.5 wt% of IL incorporation, the flow temperature of the sample decreases from 110 °C for neat zwitterionomer to 45 °C. At 11.2 wt% IL incorporation, the rubbery plateau disappears for the "cast with" sample, whereas the "swollen" sample of the same composition showed no sign of weakening in mechanical performance.

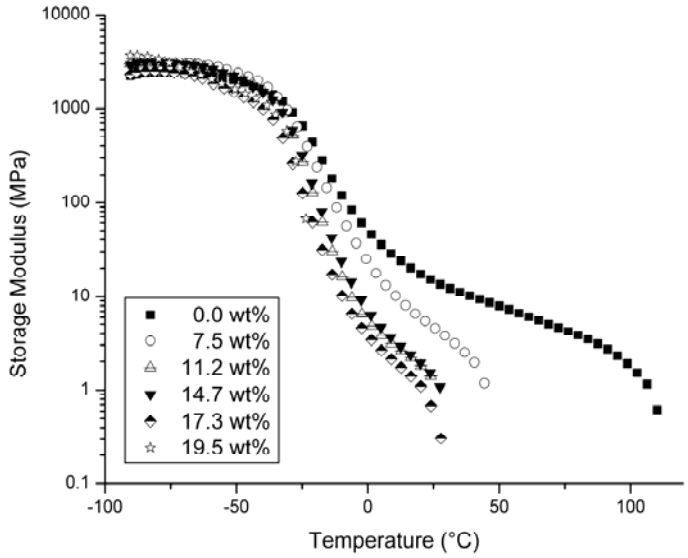

Figure 14. DMA traces of poly(*n*BA_{93}-*co*-$SBMA_7$) films cast with EMIm ES

Morphologies of Zwitterionomer/IL Composite Membranes.

To understand the different thermal mechanical behaviors of the zwitterionomer/IL composites prepared via the "swollen" method and the "cast with" method, it is necessary to probe the morphological difference between the samples. In our previous study, we employed SAXS to study the morphologies of IL-swollen zwitterionomer films. We found that the ionic peaks of the swollen samples shift to lower scattering vector "q" with increasing ionic liquid incorporation, while the shape of those ionic peaks remained unchanged.

Figure 15 overlays the SAXS traces of a neat poly(*n*BA_{91}-*co*-$SBMA_9$) film and two corresponding zwitterionomer/EMIm ES composite membranes prepared via the two IL incorporation methods. The "swollen" sample contains 14.3 wt% EMIm ES, while the "cast with" sample contains 13.6 wt% ionic liquid. As expected, both ionic peaks for the composite membranes shifted to lower "q". However, the peak shape for the "cast with" sample is much

broader than the peak for the neat sample, while the peak for the "swollen" sample remains similar to the dry sample. Preliminary SAXS results suggest that the morphology of the "cast with" sample is significantly different from either the "swollen" sample or the neat sample. While a thorough SAXS study plus modeling would be necessary to fully elucidate the morphological difference between samples prepared via the "swollen" method and the "cast with" method, we speculate that the presence of the ionic liquid molecules during film casting process of the "cast with" samples interferes with the formation of the sample morphology.

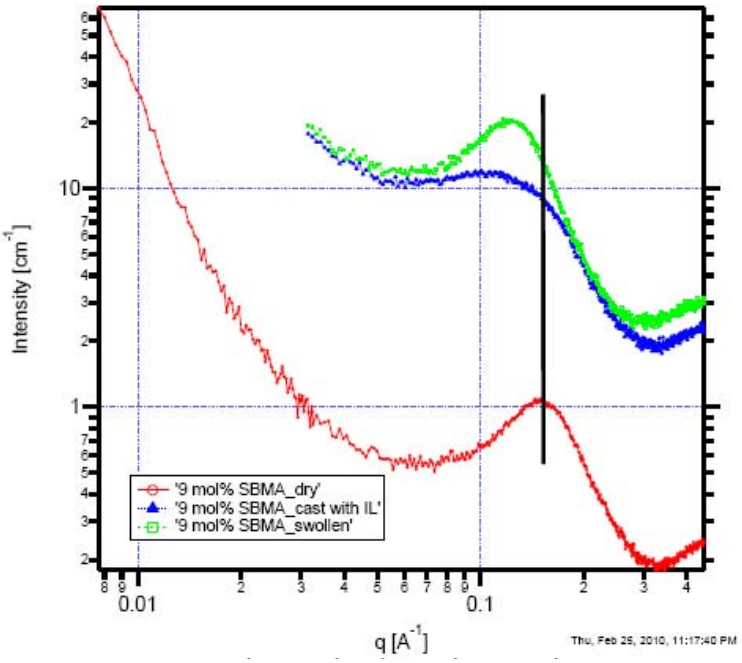

Figure 15. SAXS trace of poly(*n*BA$_{91}$-*co*-SBMA$_9$), its "swollen" sample with 14.3 wt% EMIm ES, and its "cast with" sample with 13.6 wt% EMIm ES.

Ionic Conductivities of Zwitterionomer/IL Composite Membranes.

The ionic conductivities of the zwitterionomer/IL composite membranes were measured using electrical impedance spectroscopy. **Figure 16** shows the overlaying Nyquist plots of the "cast with" samples, and the inset is an expanded image of the circled area. For both "swollen"

and “cast with” samples, single semi-circles were observed. The calculated thru-plane ionic conductivities of all samples are summarized in **Table 6**.

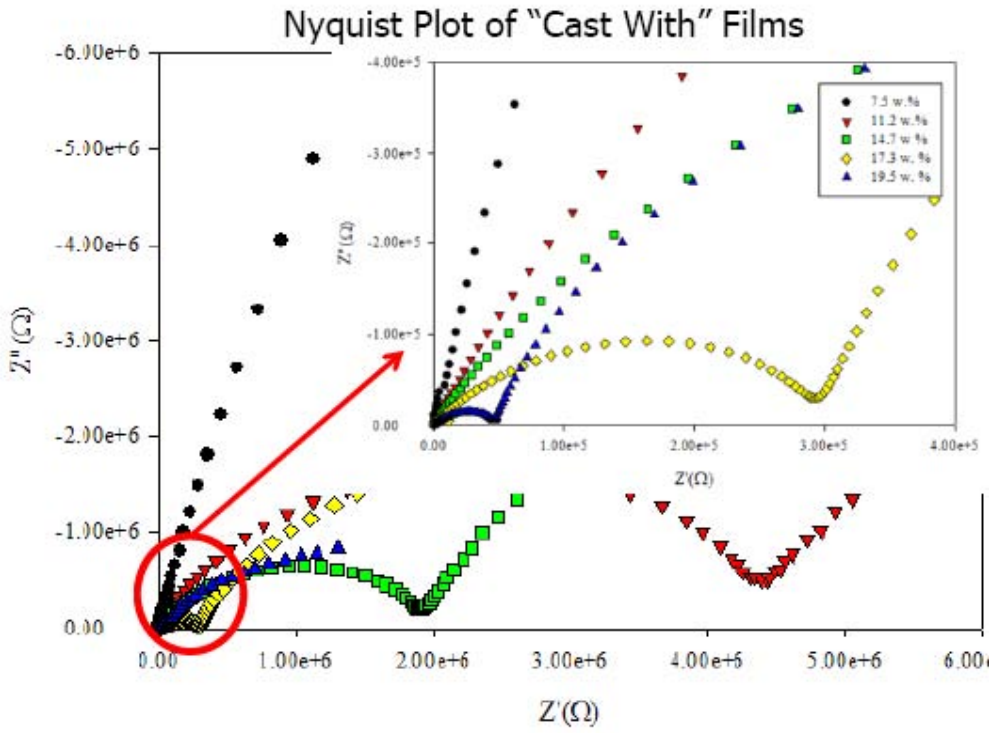

Figure 16. Nyquist plot of the “cast with” films

After adjusting for the film thickness, samples in both the “swollen” and the “cast with” category that contain higher IL contents showed higher ionic conductivities, except for the 7.7 wt% swollen sample. The possible explanation for this exception will be discussed later in this report. The ionic conductivities of the “swollen” and “cast with” samples that contain similar amounts of IL are comparable up to about 15 wt% IL incorporation. Data for “swollen” samples with higher than 13.3 wt% IL uptake will be reported in the future. Nevertheless, 3 orders of magnitude increase in the ionic conductivities of the “cast with” samples was observed between samples containing 7.5 wt% and 19.5 wt% EMIm ES. The possible scaling relationship between the ionic conductivities of these samples and their levels of IL incorporation represents of our future research focus. The fundamental understanding of the correlation between ionic

conductivity of the zwitterionomer/IL composites and their morphologies will be reported in the near future.

Table 6 Ionic conductivities of "swollen" and "cast with" zwitterionomer/IL membranes

"Swollen"		"Cast With"	
wt% of EMIm ES	σ (mS/cm)	wt% of EMIm ES	σ (mS/cm)
4.4	4.3×10^{-6}		
7.7	1.1×10^{-4}	7.5	7.6×10^{-6}
8.8	3.9×10^{-5}		
11.2	5.5×10^{-5}	11.2	8.3×10^{-5}
13.3	1.5×10^{-4}	14.7	2.0×10^{-4}
		17.3	1.3×10^{-3}
		19.5	7.5×10^{-3}

Surface Morphologies of Zwitterionomer/IL Composite Membranes

While systematic trends were observed for the thru-plane ionic conductivities of the zwitterionomer/IL membranes, the data reported here are on average 1 order of magnitude lower than our previously acquired in-plane data for the "swollen" samples.[44] The in-plane and thru-plane data should match quite well for homogeneous samples. To address this inconsistency, we analyzed the surface morphologies of our "swollen" and "cast with" membranes using optical microscopy prior to ionic conductivity measurement. Representative images are shown in **Figure 17**. We observed that the surfaces of the "cast with" samples were much smoother than those of the dry sample and the "swollen" films. The grooves observed on the surface of the "dry" sample arise from the uneven surface of the Teflon® mold, while the micro-droplets on the surfaces of the swollen films are likely ionic liquid. Such surface heterogeneity of the "swollen" samples

may explain the disagreement between our “thru-plane” and the “in-plane” data. However, a more detailed study is necessary to reach firm conclusions.

Figure 17 Optical microscopy images of a dry zwitterionomer film and two zwitterionomer/IL composite films prepared via the “swollen” method and the “cast with” method.

Conclusions

We successfully designed and synthesized BDMAEMA MS for direct comparison with SBMA. *n*BA based acrylic copolymers containing SBMA and BDMAEMA MS of varying charge compositions were polymerized. ^{1}H NMR results showed good agreement between the monomer feed and copolymer compositions. The molecular weights of the copolymers were characterized using SEC in DMF with 0.01 M LiBr, and relative values to polystyrene standards were reported. All samples used for physical and morphological characterizations are of acceptable molecular weights. The superior elastomeric performances observed for the zwitterionomers to their cationic analogs coincide with their better microphase-separated morphologies. Since the chemical structures of SBMA and BDMAEMA MS are very similar, we attributed the significantly different thermal mechanical and morphological characteristics between the corresponding copolymers to the different binding strength between the ion-ion interactions and the dipole-dipole interactions on the molecular scale. The stronger ionic

interactions in zwitterionomers may offer the potential to uptake ionic liquid, while maintaining mechanical strength, for use in advanced electro-mechanical applications.

Poly(*n*BA_{93}-*co*-$SBMA_7$)/EMIm ES composite membranes were prepared using both the "swelling" and the "cast with" methods. The "swollen" film maintained their mechanical performance with up to 14.7 wt% ionic liquid uptake, while the rubbery plateaus of "cast with" samples shortened upon EMIm ES incorporation. Preliminary SAXS results suggest that the "swollen" and the "cast with" films have different morphologies. The thru-plane ionic conductivities of the samples containing similar amounts of ionic liquid, but prepared via different methods, were comparable.

Acknowledgements

This material is based upon work supported by the U.S. Army Research Laboratory and the U.S. Army Research Office under grant number W911NF-07-1-0339. Gilles Divoux and Prof. Robert Moore in the Chemistry Department at Virginia Tech allowed the use of equipment for impedance spectroscopy and assisted with data collection and analysis. Multi-angle X-ray scattering results were provided through a collaboration with Dr. Frederick Beyer and Dr. Andrew Duncan at U.S. Army Research Laboratory.

Reference

(1) Mauritz, K. A.; Moore, R. B. *Chemical Reviews* **2004**, *104*, 4535.
(2) Hickner, M. A.; Ghassemi, H.; Kim, Y. S.; Einsla, B. R.; McGrath, J. E. *Chemical Reviews* **2004**, *104*, 4587.
(3) Ho Bum Park, Benny D. F., Zhong-Bio Zhang, Mehmet Sankir, James E. McGrath, *Angewandte Chemie International Edition* **2008**, *47*, 6019.
(4) De Smedt, S. C.; Demeester, J.; Hennink, W. E. *Pharmaceutical Research* **2000**, *17*, 113.
(5) Galin, M.; Chapoton, A.; Galin, J. C. *J. Chem. Soc. Perkin Trans.* **1993**, *2*, 545.
(6) Kudaibergenov, S.; Jaeger, W.; Laschewsky, A. *Adv. Polym. Sci.* **2006**, *201*, 157.

(7) Shi, Q.; Su, Y.; Zhao, W.; Li, C.; Hu, Y.; Jiang, Z.; Zhu, S. *Journal of Membrane Science* **2008**, *319*, 271.
(8) Zhang, Z.; Chen, S. F.; Chang, Y.; Jiang, S. Y. *Journal of Physical Chemistry B* **2006**, *110*, 10799.
(9) Cheng, N.; Brown, A. A.; Azzaroni, O.; Huck, W. T. S. *Macromolecules* **2008**, *41*, 6317.
(10) Flores, J. D.; Xu, X. W.; Treat, N. J.; McCormick, C. L. *Macromolecules* **2009**, *42*, 4941.
(11) Fevola, M. J.; Bridges, J. K.; Kellum, M. G.; Hester, R. D.; McCormick, C. L. *Journal of Applied Polymer Science* **2004**, *94*, 24.
(12) Johnson, K. M.; Fevola, M. J.; McCormick, C. L. *Journal of Applied Polymer Science* **2004**, *92*, 647.
(13) Ehrmann, M.; Muller, R.; Galin, J. C.; Bazuin, C. G. *Macromolecules* **1993**, *26*, 4910.
(14) Mathis, A.; Zheng, Y. L.; Galin, J. C. *Polymer* **1991**, *32*, 3080.
(15) Ehrmann, M.; Galin, J. C. *Polymer* **1992**, *33*, 859.
(16) Ehrmann, M.; Galin, J. C.; Meurer, B. *Macromolecules* **1993**, *26*, 988.
(17) Ehrmann, M.; Mathis, A.; Meurer, B.; Scheer, M.; Galin, J. C. *Macromolecules* **1992**, *25*, 2253.
(18) Ehrmann, M.; Mathis, A.; Meurer, B.; Scheer, M.; Galin, J. C. *Macromolecules* **1992**, *25*, 2253.
(19) Ehrmann, M.; Muller, R.; Galin, J. C.; Bazuin, C. G. *Macromolecules* **1993**, *26*, 4910.
(20) Gauthier, M.; Carrozzella, T.; Snell, G. *Journal of Polymer Science Part B-Polymer Physics* **2002**, *40*, 2303.
(21) Koberle, P.; Laschewsky, A. *Macromolecules* **1994**, *27*, 2165.
(22) Galin, M.; Marchal, E.; Mathis, A.; Meurer, B.; Soto, Y. M. M.; Galin, J. C. *Polymer* **1987**, *28*, 1937.
(23) Galin, M.; Marchal, E.; Mathis, A.; Galin, J. C. *Polym. Adv. Technol.* **1997**, *8*, 75.
(24) Lu, J. M.; Yan, F.; Texter, J. *Prog. Polym. Sci.* **2009**, *34*, 431.
(25) Agrawal, R. C.; Pandey, G. P. In *Meeting on Photorefractive Effects and Devices* Lake Tahoe, CA, 2008.
(26) Luo, S. C.; Zhang, Z. X.; Yang, L. *Chin. Sci. Bull.* **2008**, *53*, 1337.
(27) Galinski, M.; Lewandowski, A.; Stepniak, I. *Electrochimica Acta* **2006**, *51*, 5567.
(28) Lee, C. P.; Lee, K. M.; Chen, P. Y.; Ho, K. C. In *17th International Materials Research Congress* Cancun, MEXICO, 2008, p 1411.
(29) Yang, S. C.; Yoon, H. G.; Lee, S. S.; Lee, H. *Mater. Lett.* **2009**, *63*, 1465.
(30) Mishra, A.; Fischer, M. K. R.; Bauerle, P. *Angew. Chem., Int. Ed.* **2009**, *48*, 2474.
(31) Bennett, M. D.; Leo, D. J.; Wilkes, G. L.; Beyer, F. L.; Pechar, T. W. *Polymer* **2006**, *47*, 6782.
(32) Ding, J.; Zhou, D.; Spinks, G.; Wallace, G.; Forsyth, S.; Forsyth, M.; MacFarlane, D. *Chem. Mater.* **2003**, *15*, 2392.
(33) Lu, W.; Fadeev, A. G.; Qi, B.; Smela, E.; Mattes, B. R.; Ding, J.; Spinks, G. M.; Mazurkiewicz, J.; Zhou, D.; Wallace, G. G.; MacFarlane, D. R.; Forsyth, S. A.; Forsyth, M. *Science* **2002**, *297*, 983.
(34) Vidal, F.; Plesse, C.; Teyssie, D.; Chevrot, C. *Synth. Met.* **2004**, *142*, 287.
(35) Bennett, M. D.; Leo, D. J. *Sens. Actuators, A* **2004**, *115*, 79.
(36) Galin, M.; Mathis, A.; Galin, J. C. *Macromolecules* **1993**, *26*, 4919.
(37) Hamid, S. M.; Sherrington, D. C. *Polymer* **1987**, *28*, 325.

(38) Oya, T.; Kunita, K.; Araki, K.; Iwai, Y.; Sonokawa, K.; Sasaki, T.; (Fujifilm Corporation, Japan). Application: EP, 2008, p 118pp.
(39) Ushakova, V. N.; Kipper, A. I.; Afanakina, N. A.; Samarova, O. E.; Klenin, S. I.; Panarin, E. F. *Vysokomolekulyarnye Soedineniya, Seriya A i Seriya B* **1995**, *37*, 933.
(40) Yuan, H.; Li, C.; Zhu, Y.; Huang, B.; (Shanghai Hengyi Chemical Co., Ltd., Peop. Rep. China). Application: CN, 2006, p 12pp.
(41) Layman, J. M.; Borgerding, E. M.; Williams, S. R.; Heath, W. H.; Long, T. E. *Macromolecules* **2008**, *41*, 4635.
(42) Burch, R. R.; Manring, L. E. *Macromolecules* **1991**, *24*, 1731.
(43) Strehmel, V.; Wetzel, H.; Laschewsky, A.; Moldenhauer, E.; Klein, T. *Polym. Adv. Technol.* **2008**, *19*, 1383.
(44) Brown, R. H.; Duncan, A. J.; Choi, J. H.; Park, J. K.; Wu, T. Y.; Leo, D. J.; Winey, K. I.; Moore, R. B.; Long, T. E. *Macromolecules* **2010**, *43*, 790.